Published OnlineFirst May 11, 2010; DOI: 10.1158/0008-5472.CAN-09-3791
Published OnlineFirst on May 11, 2010 as 10.1158/0008-5472.CAN-09-3791

Cancer Research

A Novel Senescence-Evasion Mechanism Involving Grap2 and Cyclin D Interacting Protein Inactivation by Ras Associated with Diabetes in Cancer Cells under Doxorubicin Treatment

Inkyoung Lee[1], Seon-Yong Yeom[1], Sook-Ja Lee[1], Won Ki Kang[1,2], and Chaehwa Park[1,2]

Abstract

Ras associated with diabetes (Rad) is a Ras-related GTPase that promotes cell growth by accelerating cell cycle transitions. Rad knockdown induced cell cycle arrest and premature senescence without additional cellular stress in multiple cancer cell lines, indicating that Rad expression might be critical for the cell cycle in these cells. To investigate the precise function of Rad in this process, we used human Rad as bait in a yeast two-hybrid screening system and sought Rad-interacting proteins. We identified the Grap2 and cyclin D interacting protein (GCIP)/DIP1/CCNDBP1/HHM, a cell cycle–inhibitory molecule, as a binding partner of Rad. Further analyses revealed that Rad binds directly to GCIP *in vitro* and coimmunoprecipitates with GCIP from cell lysates. Rad translocates GCIP from the nucleus to the cytoplasm, thereby inhibiting the tumor suppressor activity of GCIP, which occurs in the nucleus. Furthermore, in the presence of Rad, GCIP loses its ability to reduce retinoblastoma phosphorylation and inhibit cyclin D1 activity. The function of Rad in transformation is also evidenced by increased telomerase activity and colony formation according to Rad expression level. *In vivo* tumorigenesis analyses revealed that tumors derived from Rad knockdown cells were significantly smaller than those from control cells (P = 0.0131) and the preestablished tumors are reduced in size after the injection of siRad (P = 0.0064). Therefore, we propose for the first time that Rad may promote carcinogenesis at least in part by inhibiting GCIP-mediated tumor suppression. *Cancer Res; 70(11); OF1–9. ©2010 AACR.*

Introduction

Subtractive hybridization initially identified the gene encoding Ras associated with diabetes (Rad) as being overexpressed in type II diabetic muscle (1, 2). Rad is a 35-kDa Ras-related GTPase encoded by a gene located at human chromosome 16q22 (1). Rad differs from the other Ras-related GTPases in several properties, including its lack of several characteristic domains including prenylation motifs, a GTP-binding domain, and NH_2- and COOH-terminal extensions (3). Rad is a nonlipid-dependent cytosolic protein (3) that is overexpressed in tumor tissue, interacts with nm23, and is associated with poor prognosis of breast cancer patients (4). Rad participates in Ca^{2+}-triggered signaling events, such as the CaMKII serine/threonine kinase cascade, in which it interacts with calmodulin (5), calmodulin-dependent protein kinase II (5), and tropomyosin (6). Previously, Tseng and colleagues reported that Rad promotes cell growth by accelerating cell cycle transitions (4). However, the exact function of Rad in the cell cycle is not yet known.

Senescence, which is defined as an irreversible cell cycle arrest, is an inherent tumor suppression mechanism (7, 8). In the process of identifying senescence-associated genes, we found that Rad was significantly suppressed in cancer cells that had undergone doxorubicin-induced cell cycle arrest. Notably, knockdown of Rad resulted in cell cycle arrest and premature senescence without additional cellular stress in multiple cancer cells. To investigate the connection between Rad knockdown and cell cycle arrest, we screened for intracellular molecules capable of interacting with Rad.

This study presents results showing a novel physical interaction between Rad and the Grap2 and cyclin D interacting protein (GCIP; ref. 9). GCIP is a human homologue of the MAID protein and the D-type cyclin–interacting protein 1. GCIP is a 40-kDa helix-loop-helix leucine zipper protein (10, 11) that is expressed mainly in terminally differentiated tissues (10), with lower expression levels observed in human breast, prostate, and colon tumor tissues (12). The gene encoding GCIP is located on chromosome 15q15, which is frequently deleted in tumor tissues, including those of the colon, breast, lung, and bladder (13). GCIP is known to interact with Grap2 (9), cyclin D1 (9), and SirT6 (12), and has been shown to inhibit the transcriptional activity of the cyclin D1 promoter,

Authors' Affiliations: [1]Biomedical Research Institute, Samsung Medical Center and [2]Department of Medicine, Sungkyunkwan University School of Medicine, Seoul, Korea

Note: Supplementary data for this article are available at Cancer Research Online (http://cancerres.aacrjournals.org/).

Corresponding Authors: Chaehwa Park or Won Ki Kang, Department of Medicine, Samsung Medical Center, Sungkyunkwan University School of Medicine, 50 Irwon-Dong, Seoul, 135-710, Korea. Phone: 82-2-3410-3458; Fax: 82-2-3410-1757; E-mail: cpark@skku.edu or wkkang@skku.edu.

doi: 10.1158/0008-5472.CAN-09-3791

©2010 American Association for Cancer Research.

Downloaded from cancerres.aacrjournals.org on April 20, 2017. © 2010 American Association for Cancer Research.

Published OnlineFirst May 11, 2010; DOI: 10.1158/0008-5472.CAN-09-3791

decrease the phosphorylation of the retinoblastoma (Rb) protein at Ser780, slow cell cycle progression, and decrease susceptibility to carcinogenesis (10, 11, 14, 15).

In the present study, we explored the role of Rad in regulating cellular senescence and sought to identify some of the involved mechanisms. Specifically, we investigated the effects of Rad expression on the cellular response to DNA-damaging agents. Our results revealed that Rad expression led to decreased senescence and increased doxorubicin resistance. Furthermore, Rad expression downregulated multiple genes involved in growth arrest or senescence, and decreased the protein levels of p27 in doxorubicin-treated cells. Telomerase activity and colony formation were increased by Rad expression and *in vivo* tumorigenesis in athymic nude mice was found to differ based on the Rad expression level of the tumorigenic cells. Finally, we showed for the first time that Rad interacts with GCIP, and inhibits GCIP-mediated decreases in cyclin D activity and Rb phosphorylation, which are critical for both the cell cycle and senescence (16). Based on these novel findings, we propose that this function of Rad may significantly contribute to tumor progression through the inhibition of senescence.

Materials and Methods

Cell lines, reagents, and plasmids

293T cells were grown in DMEM (Life Technologies Life Science). Human prostate (PC-3, DU145, and LNCaP), stomach (SNU638, MKN74, and SNU668), and breast (MDA-MB468) cancer cells were grown in RPMI (Life Technologies Life Science). Normal human prostate epithelial cells (PrEC), purchased from Lonza, were grown in PeEBM (Lonza). Immortalized (RWPE-1) and transformed (RWPE-2) prostate epithelial cells obtained from the American Type Culture Collection were grown in K-SFM (Life Technologies). All constructs were generated by PCR using primers designed from the coding regions of the relevant human cDNAs. The full-length Rad open reading frame was cloned from HeLa mRNA for Flag-tagged cloning into pCMVTaq2B (Clonetech). HA-tagged-GCIP constructs were ligated into pCMVTaq4C (Clonetech). Stable cell lines overexpressing Rad were selected with changes of fresh medium containing G418 (600 μg/mL). Rad-targeting small interfering RNA (siRNA) and control siRNA were obtained from Dharmacon. Cells were transfected with siRNA or plasmids using Effectine (Qiagen) or the Amaxa electroporation system (Amaxa), according to the supplier's protocol. Antibodies against Rb, p21, p27, E2F-1, cyclin A, cdc2, cyclin D1, Flag, and β-actin were obtained from Santa Cruz Biotechnology. Antibodies against pRb^{S780} and Rad were purchased from Cell Signaling and Abnova, respectively.

Yeast two-hybrid analysis

Yeast two-hybrid screening with human Rad was performed with the activation domain (AD)-tagged HeLa cDNA library. Yeast strain PBN204 (Panbionet) was cotransformed with two hybrid plasmids, a bait plasmid pBCT-Rad that encodes a GAL4 DNA BD-fused Rad cDNA, and a pACT2 plasmid that encodes the human HeLa cell cDNA fused to GAL4 AD. Three different reporter genes, *URA3, ADE2*, and *lacZ*, each of which was under the control of different GAL4-binding sites, were used to minimize false positives. The transformants were spread on selective media lacking leucine, tryptophan, and uracil and containing 2% glucose (SD-LWU), in which the transformants can grow when BD-Rad interacts with AD-prey proteins. One hundred thirty-five independent colonies grew on selective media SD-LWU. Colonies grew on selective media lacking leucine, tryptophan, and adenine, and containing 2% glucose (SD-LWA). Colonies showed a blue color in 5-bromo-4-chloro-3-indolyl-β-D-galactopyranoside, which was confirmed by filter assay to allow for the detection of β-galactosidase expression. pBCT-polypyrimidine tract binding protein and pACT2-polypyrimidine tract binding protein served as the positive control for the protein-protein interaction (17). pBCT (Panbionet) and pACT2 (Clontech) were used as the negative control.

In vitro transcription, translation, and glutathione *S*-transferase pull-down assay

The Rad cDNA was in-frame cloned into pGEX4T-1 (Amersham) to produce the glutathione *S*-transferase (GST) fusion proteins for GST-pull-down assay. GST, GST-Rad fusion proteins were immobilized on glutathione-Sepharose beads (Amersham) and incubated with normalized 10 μL of GCIP labeled with [^{35}S]methionine in a buffer [50 mmol/L HEPES (pH 7.6), 50 mmol/L NaCl, 5 mmol/L EDTA, 0.1% NP40, and 10% glycerol]. The beads were then washed and the bound proteins were eluted with the SDS-loading buffer containing 5% β-mercaptoethanol and subjected to SDS-PAGE followed by autoradiography. GCIP labeled with [^{35}S]methionine was prepared by subcloning cDNA into pcDNA3.1(+) (Invitrogen) and *in vitro* translation using the TNT quick-coupled rabbit reticulocyte system (Promega) according to the manufacturer's instructions.

Immunoprecipitation

For immunoprecipitation, 293T cells were transfected with pFlag-Rad or pHA-GCIP, washed with cold PBS, and lysed in a buffer [20 mmol/L HEPES (pH 7.0), 150 mmol/L NaCl, 1 mmol/L EDTA, 2 mmol/L β-glycerophosphate, 1% Triton X-100, 10% glycerol, 1 mmol/L phenylmethylsulfonyl fluoride, and 1× protease inhibitor cocktail]. The cell lysates underwent centrifugation at 14,000 *g* at 4°C for 15 minutes. Anti-HA antibody (Cell Signaling) was incubated with protein G-agarose overnight in PBS at 4°C. The immunecomplexes were washed four times with lysis buffer and analyzed by SDS-PAGE, followed by Western blotting.

Immunofluorescence

Cells (293T) were transfected with plasmids using Effectine. After 24 hours, cells were fixed with 3.7% formaldehyde in PBS buffer, permeabilized with 0.2% Triton X-100, and blocked in PBS containing 5% bovine serum albumin. Fixed cells were then incubated with primary antibodies overnight, washed with PBS, and incubated with the secondary antibodies conjugated to either Alexa 488 or

Downloaded from cancerres.aacrjournals.org on April 20, 2017. © 2010 American Association for Cancer Research.

Published OnlineFirst May 11, 2010; DOI: 10.1158/0008-5472.CAN-09-3791

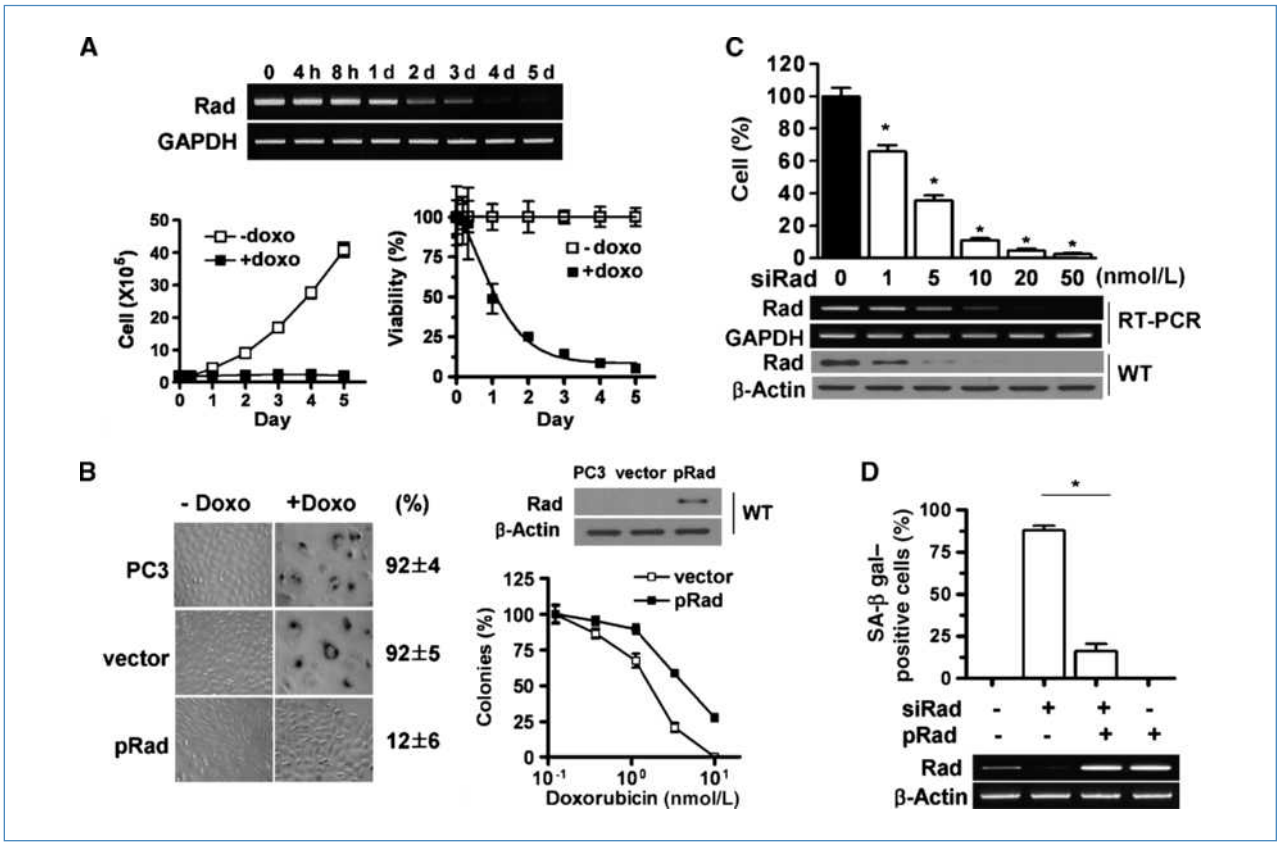

Figure 1. Rad is associated with a cell cycle arrest. A, reverse transcription-PCR (RT-PCR) analysis of Rad in PC-3 cells during doxorubicin (doxo; 10 nmol/L) treatment. Bottom, the kinetics of growth arrest induced by doxorubicin. GAPDH, glyceraldehyde-3-phosphate dehydrogenase. B, induction of senescence by low-dose of doxorubicin. Left, after culturing with doxorubicin for 5 d, the cells were stained for SA-β-Gal. Number on the right, the percentage of SA-β-Gal–positive cells. Right, cells (2×10^2) were seeded in 60-mm dishes and incubated in the presence of the indicated concentrations of doxorubicin. After 2 wk, colonies were counted under a phase-contrast microscope. C, effects of siRad on the growth of PC-3 cells. siRad- and siC-transfected PC-3 cells were analyzed by trypan blue staining 5 d after transfection. *, $P < 0.05$ versus siC. WT, wild-type. D, expression of Rad rescued siRad-induced senescence. *, $P < 0.05$. The cells were stained for SA-β-Gal activity 3 d after transfection.

Alexa 594. Primary antibodies used were rabbit anti-HA (1:200) and mouse anti-Flag (1:500). Secondary antibodies were anti-rabbit Alexa 488 (1:500) and anti-mouse Alexa 594 (1:500). 4′,6′-Diamino-2-phenylindole (DAPI) was used to stain the nuclei. Confocal scanning analysis of the cells was done with RADIANCE 2100 confocal imaging system (Bio-Rad).

Cyclin D1 promoter and Rb phosphorylation reporter assays

To examine the influence of Rad and GCIP on cyclin D1 and Rb activity, pGL3-cyclin D1-Luc and ppRb-TA-Luc (Clontech), which contained the luciferase gene under the control of a cyclin D1– and a phosphorylated Rb–responsive element, were used. For Rb phosphorylation reporter assays, cells were transfected with either empty vector pHA-GCIP, pFlag-Rad, or a combination of plasmids together with luciferase vector. After 48 hours, the cells were lysed and luciferase activity was determined according to the supplier's protocol (Promega). Luciferase activity is given as mean ± SD of triplicated experiments.

In vivo tumorigenesis

To examine the effect of Rad expression in tumor formation, 1.5×10^6 PC-3 cells were implanted s.c. into 4-week-old female BALB/c nude mice and the tumor growth was monitored using calipers every 3 to 4 days. For a treatment model, exponentially growing PC-3 cells (1.5×10^6/injection) were implanted s.c. into the nude mice for tumor formation. When tumors reached an average size of 40 to 50 mm^3 (~4 wk), mice were divided into two groups: siControl (siC) and siRad. The mice received two (day 1 and day 7) intratumoral injections of siRNA as a mixture of siRNA (50 nmol/L) in 100 μL of Effectene per injection. Tumor volume was calculated using the formula $(a \times b^2) \times 0.5$, in which a is a long axis and b is a short axis in millimeters. All mice were obtained from the Charles River Laboratory, maintained and sacrificed according to institutional guidelines, and the procedures were approved by the Institutional Committee on the Use and Care of Animals and Recombinant DNA research.

Statistical analysis

Data presented in the graphs represent a mean ± SD of the values from at least three independent measurements. To

Downloaded from cancerres.aacrjournals.org on April 20, 2017. © 2010 American Association for Cancer Research.

Published OnlineFirst May 11, 2010; DOI: 10.1158/0008-5472.CAN-09-3791

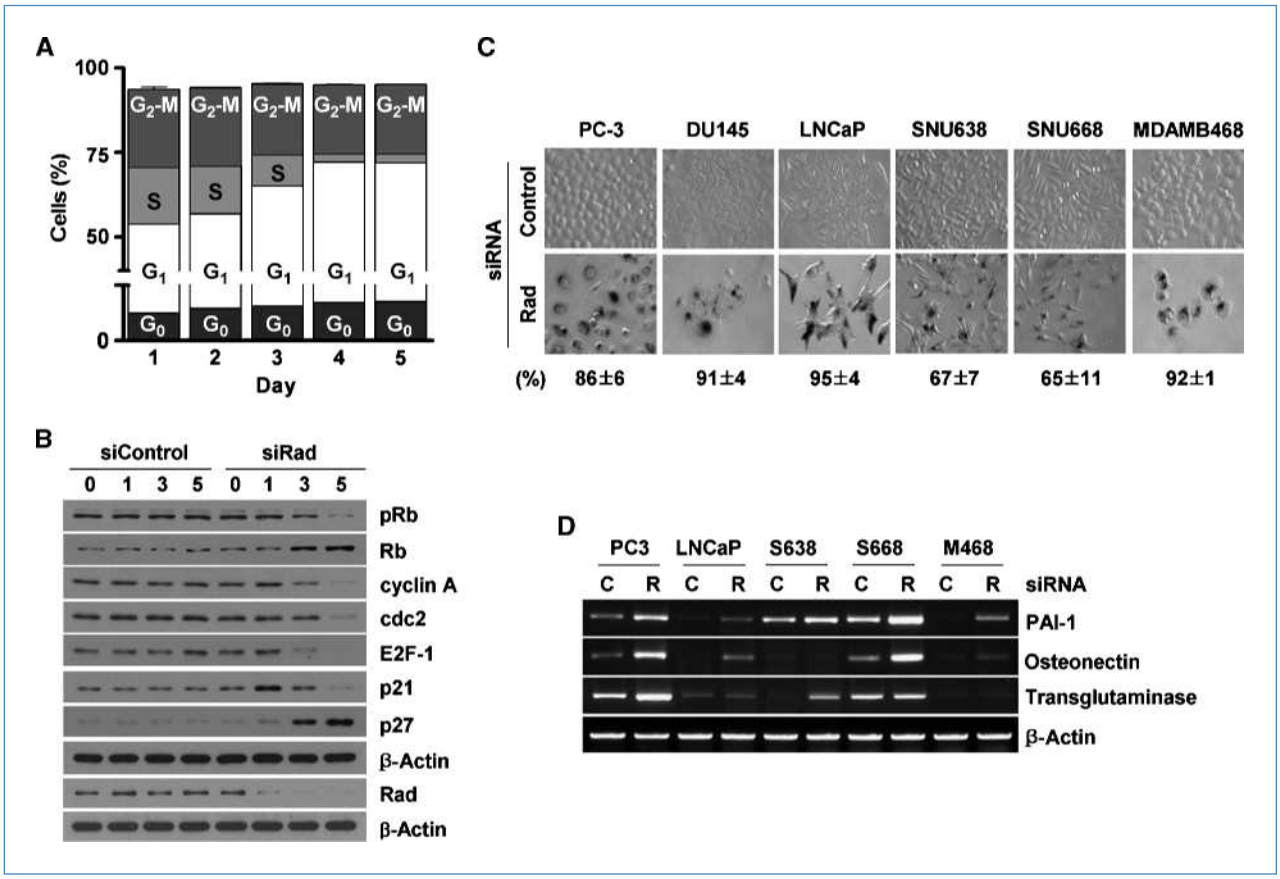

Figure 2. Rad knockdown induces cell cycle arrest and premature senescence but not cell death. A, effect of Rad knockdown on the cell cycle distribution of PC-3 cells. Cell cycle analysis was done by flow cytometry following propidium iodide staining. B, changes in the expression of cell cycle–related proteins following siRNA transfection. C, siRad induced senescence in multiple cancer cells (PC-3, DU145, and LNCaP prostate cancer cells; MKN74, SNU638, and SNU668 stomach cancer cells; and MDA-MB468 breast cancer cells). Cells were stained for SA-β-Gal 5 d after transfection of siRNAs (50 nmol/L). The numbers indicate the percentage of SA-β-Gal–positive cells. D, RT-PCR analysis of senescence-associated genes in multiple cancer cells. The cDNAs of Rad, PAI-1, osteonectin, and transglutaminase were amplified by PCR using primers designed from the coding region of the human cDNA (Supplementary Table S2).

test the difference in mean values, Student's t test was applied. Intergroup comparison was made with a paired two-sample t test. The difference was considered significant if the P value was <0.05.

Results

Identification of Rad as a cell cycle–associated molecule

Doxorubicin is an anticancer agent frequently used to treat a variety of solid tumors and triggers DNA damage–induced premature senescence (8, 18, 19). Low-dose doxorubicin reduced Rad expression (Fig. 1A, top) and induced a senescence-like growth arrest 5 days after the treatment in PC-3 human prostate carcinoma cells (Fig. 1A, bottom), as evidenced by flat, enlarged, SA-β-Gal–positive cells (Fig. 1B, left). However, overexpression of Rad prevented the doxorubicin-induced growth arrest (Supplementary Fig. S1A; Fig. 1B, left) and improved cell growth compared with doxorubicin-treated control cells (Supplementary Fig. S1B). These results indicate that Rad suppresses DNA damage–induced cell cycle arrest and induction of premature senescence in PC-3 cells. Importantly, a clonogenic survival assay revealed a shift in the doxorubicin dose response among Rad-overexpressing cells (Fig. 1B, right), indicating that Rad expression increased doxorubicin resistance.

We next examined whether the decrease of Rad might be related to this drug-induced cell growth inhibition. An assay of cell viability using trypan blue staining revealed that siRad specifically inhibited cell growth, whereas the control siRNA did not (Fig. 1C). Notably, the cell growth inhibition was siRad dose dependent. As shown in Fig. 1D, Rad overexpression effectively rescued cells from siRad-induced premature senescence, indicating that these biological changes were Rad mediated.

Rad knockdown induces cell cycle arrest and senescence

We next examined the effect of siRad on the cell cycle progression of PC-3 cells. Knockdown of Rad significantly arrested cell growth inducing premature senescence, compared with siC-treated cells, and the percentage of SA-β-Gal–positive cells increased gradually until the 5th day after siRad transfection (Supplementary Fig. S2A and B). As

Downloaded from cancerres.aacrjournals.org on April 20, 2017. © 2010 American Association for Cancer Research.

Published OnlineFirst May 11, 2010; DOI: 10.1158/0008-5472.CAN-09-3791

shown in Supplementary S2A and Fig. 2A, siRad-transfected cells were arrested in the G_1 phase of the cell cycle. Propidium iodide/Annexin staining (Supplementary Fig. S3A) and terminal deoxynucleotidyl transferase–mediated dUTP nick end labeling assays (Supplementary Fig. S3B and C) confirmed that siRad-transfected cells failed to undergo cell death by either apoptosis or necrosis.

Senescence is defined as irreversible growth arrest, which is associated with cell cycle inhibitors (20, 21). Rad knockdown increased the level of p27 and decreased Rb phosphorylation; these effects were accompanied by a decrease in the S-phase proteins cdc2, cyclinA, and E2F1 (Fig. 2B).

To test whether Rad knockdown–induced senescence is a general phenomenon in cancer cells derived from different tissues, several cell lines were evaluated for Rad expression and siRad-induced senescence. The tested cancer cells from different tumor tissues displayed senescence after transfection with siRad (Fig. 2C). Previously, we reported that doxorubicin induced senescence in PC-3 and LNCaP cells but not in DU145 cells (22, 23). However, DU145 cells, which contain mutated forms of p53, pRb, and p16, developed senescence in response to Rad knockdown, which is consistent with previous studies (8, 24) showing premature senescence in breast tumor cells and colon cancer cells that lack functional p16. The previously reported senescence marker proteins PAI-1 (25), osteonectin (26), and transglutaminase (27) were increased in some cell lines after Rad knockdown in the tested diverse cancer cell lines (Fig. 2D), providing further confirmation of senescence induction by Rad knockdown.

Rad interacts with GCIP and induces its translocation from the nucleus to the cytoplasm

To define the precise mechanism of Rad-mediated cell cycle control, we used the full-length Rad cDNA as bait in a yeast two-hybrid system, screened a HeLa cDNA library, and identified several clones that seemed to specifically interact with Rad. DNA sequencing and basic alignment searches of the National Center for Biotechnology Information database allowed us to identify one of the positive clones as corresponding to GCIP (Fig. 3A), which was previously reported as a cell cycle inhibitory molecule (13, 14). To examine whether GCIP is able to interact with Rad in mammalian cells, we transfected GCIP-HA or Rad-encoding expression vectors into human 293T cells and performed immunoblot analysis. As shown in Fig. 3B, Rad was detected by Western blot analysis after coimmunoprecipitation with an

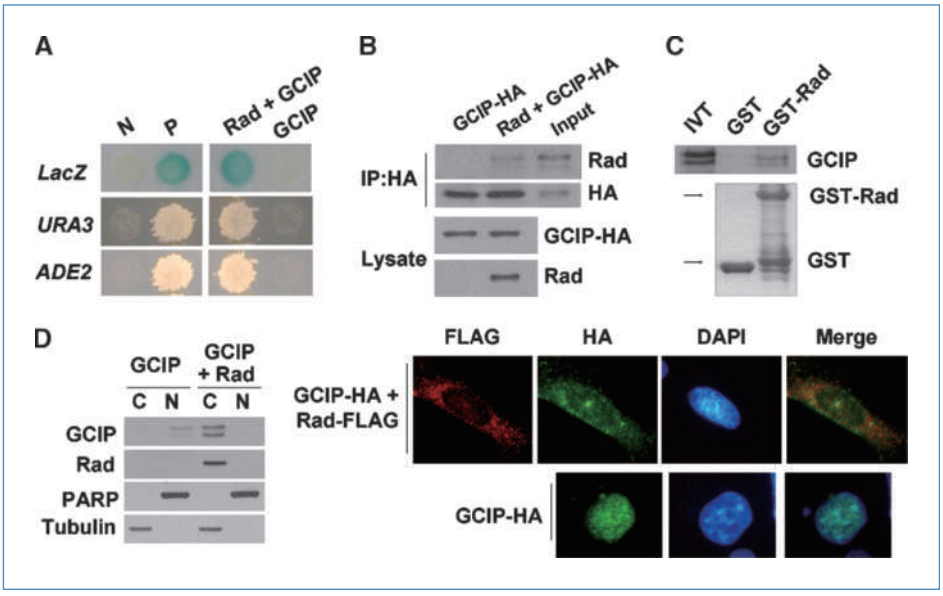

Figure 3. Rad interacts with GCIP *in vitro* and *in vivo*. A, identification of GCIP as a Rad-interacting molecule by yeast two-hybrid screening. Yeast strain PBN204 was cotransformed with the GAL4-BD fusion plasmid pBCT or pBCT-Rad, and GAL4-AD fusion plasmid pACT2 or pACT2-GCIP. Transformants were streaked on selective media SD-LWU, SD-LWA, and a SD medium containing 5-bromo-4-chloro-3-indolyl-β-D-galactopyranoside. When two proteins interact with each other, cotransformants will express lacZ, URA3, and Ade2. P, positive control; N, negative control. B, coimmunoprecipitation (IP) of GCIP with Rad. Total cell lysates from Rad-transfected 293T cells were immunoprecipitated with anti-HA antibody and the presence of Rad in the immunoprecipitates was detected by Western blotting using anti-Rad antibody. C, binding of GST-fused recombinant Rad to full-length ^{35}S-GCIP. The GST-Rad fusion protein was expressed in *Escherichia coli* and purified. Equal amounts of *in vitro* translated ^{35}S-radiolabeled GCIP were incubated with GST alone or GST-Rad fusion proteins. Bound proteins were collected on GST- Sepharose beads, and proteins were resolved by SDS-PAGE and analyzed by autoradiography. Coomassie-stained GST fusion proteins from the same gel are aligned to show protein levels. D, cytoplasmic colocalization of HA-GCIP and Rad-Flag. 293T cells were transfected with vectors encoding Rad and GCIP. Left, cytoplasmic (C) and nuclear (N) fractions were prepared and 30 μg of proteins from each fraction were subjected to Western blot analysis using anti-GCIP or anti-Rad antibody. Right, cytoplasmic colocalization of HA-GCIP and Rad-Flag. Merged image of Rad (red), GCIP (green), and DAPI-stained DNA (blue) clearly shows colocalization of GCIP with Rad.

Downloaded from cancerres.aacrjournals.org on April 20, 2017. © 2010 American Association for Cancer Research.

Published OnlineFirst May 11, 2010; DOI: 10.1158/0008-5472.CAN-09-3791

anti-HA antibody. The results revealed that Rad specifically interacted with GCIP. Coimmunoprecipitation assays with *in vitro* translated GCIP and recombinant GST-Rad revealed that the GCIP protein directly interacted with GST-Rad but not with GST alone (Fig. 3C). To examine where the GCIP-Rad binding may occur in cells, we fractionated cell lysates from 293T cells transfected with Rad and/or GCIP, and subjected cytoplasmic and nuclear fractions to immunoblot analysis. The results indicated that Rad was present mainly in the cytoplasm, whereas GCIP was translocated from the nucleus to the cytoplasm in the presence of Rad (Fig. 3D, left). To further investigate whether GCIP associates with Rad *in vivo*, we transfected 293T cells with GCIP alone, or Rad and GCIP, and subjected the cells to immunofluorescent staining. Consistent with a previous report (28), GCIP transfectants showed fluorescence almost exclusively in the nucleus (Fig. 3D, right). Notably, however, cotransfection of Rad with GCIP resulted in the translocation of GCIP from the nucleus to the cytoplasm (Fig. 3D). Rad-induced GCIP translocation was also observed in PC-3 cells (Supplementary Fig. S4).

GCIP-mediated inhibition of Rb phosphorylation and cyclin D1 is repressed by Rad

To determine whether the interaction between GCIP and Rad has any effect on GCIP-modulated Rb phosphorylation and cyclin D1 activation, we cotransfected 293T cells with Rad- or GCIP-expressing plasmids plus ppRb-TA-Luc or pGL3-cyclin D1-Luc. As shown in Fig. 4A and B, the activities of both reporters were decreased in cells transfected with the plasmid encoding GCIP (lane 1 versus 2; ppRb-TA-Luc, $P = 0.001$; pGL3-cyclin D1-Luc, $P = 0.0008$) but not with that encoding Rad (lane 1 versus 3, $P > 0.05$). Cotransfection of vectors encoding both Rad and GCIP relieved the downregulation of the reporter activities seen in GCIP-expressing cells (lane 2 versus 4, $P < 0.0001$). To further confirm the inactivation of GCIP by Rad in carcinoma cells, we performed the same experiment using PC-3 cells. As shown in Supplementary Fig. S5, expression of recombinant GCIP downregulated Rb phosphorylation and cyclin D1 activity in PC-3 cells expressing GCIP alone ($P = 0.002$ and $P = 0.001$, respectively), but not in PC-3 cells coexpressing Rad (lane 3 versus 4, $P > 0.05$).

Rad overexpression increases cyclin D1 expression and Rb phosphorylation

Because GCIP has been reported to inhibit the expression of cyclin D1 (13), we examined whether Rad overexpression might enhance cyclin D1 levels. Western blot analysis showed that cyclin D1 expression was increased in Rad-overexpressing 293T cells (Fig. 4C, top). In addition, phosphorylation of Rb at Ser780, a site exclusively phosphorylated by cyclin D1-Cdk4 (29), was also enhanced in Rad-expressing

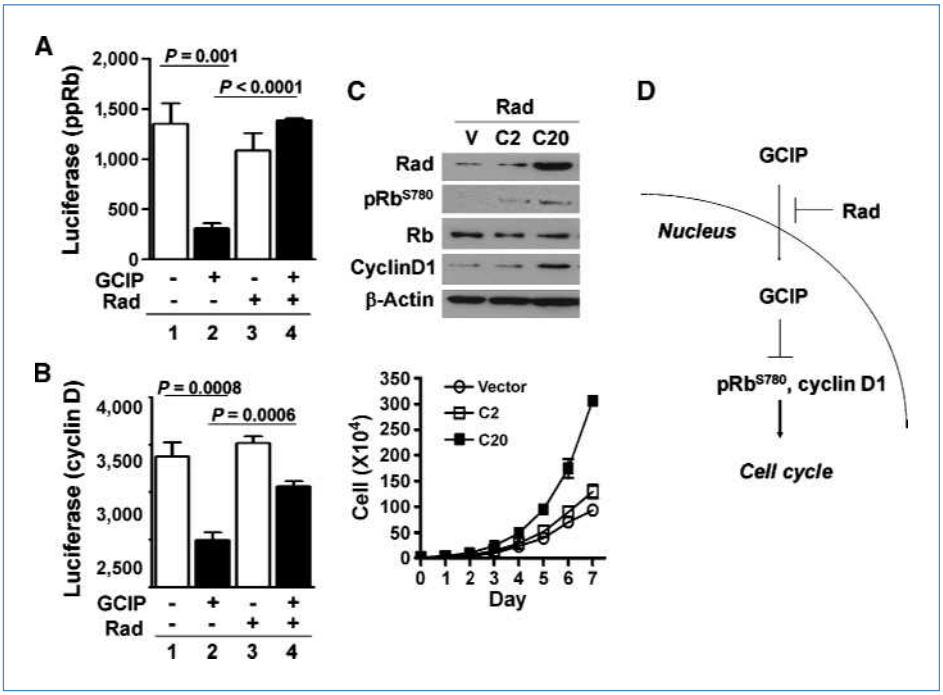

Figure 4. GCIP-mediated inhibition of cyclin D and Rb phosphorylation is repressed by Rad. Rad modulates GCIP-mediated inhibition of Rb phosphorylation (A) and cyclin D promoter luciferase activity (B). 293T cells (5×10^4) were transiently transfected with empty control vector (50 ng), pHA-GCIP (50 ng), pFlag-Rad (50 ng), or a combination (1:1 ratio) of expression plasmids together with 100 ng of luciferase vector. C, Rad-overexpressing cells exhibit increased cyclin D1 and pRb^{S780}. Cell lysates from 293T-derivative transfectants were separated from SDS-PAGE followed by immunoblotting (top). Bottom, expression of Rad enhances 293T cell proliferation. Stable 293T cell clones (1×10^2) were seeded in six-well culture plates. At the indicated times, cells in triplicate wells were analyzed using trypan blue staining. D, a model based on our studies illustrates that Rad inhibits GCIP by cytoplasmic sequestration, thereby increasing the levels of cyclin D1 expression and Rb phosphorylation.

Downloaded from cancerres.aacrjournals.org on April 20, 2017. © 2010 American Association for Cancer Research.

Published OnlineFirst May 11, 2010; DOI: 10.1158/0008-5472.CAN-09-3791

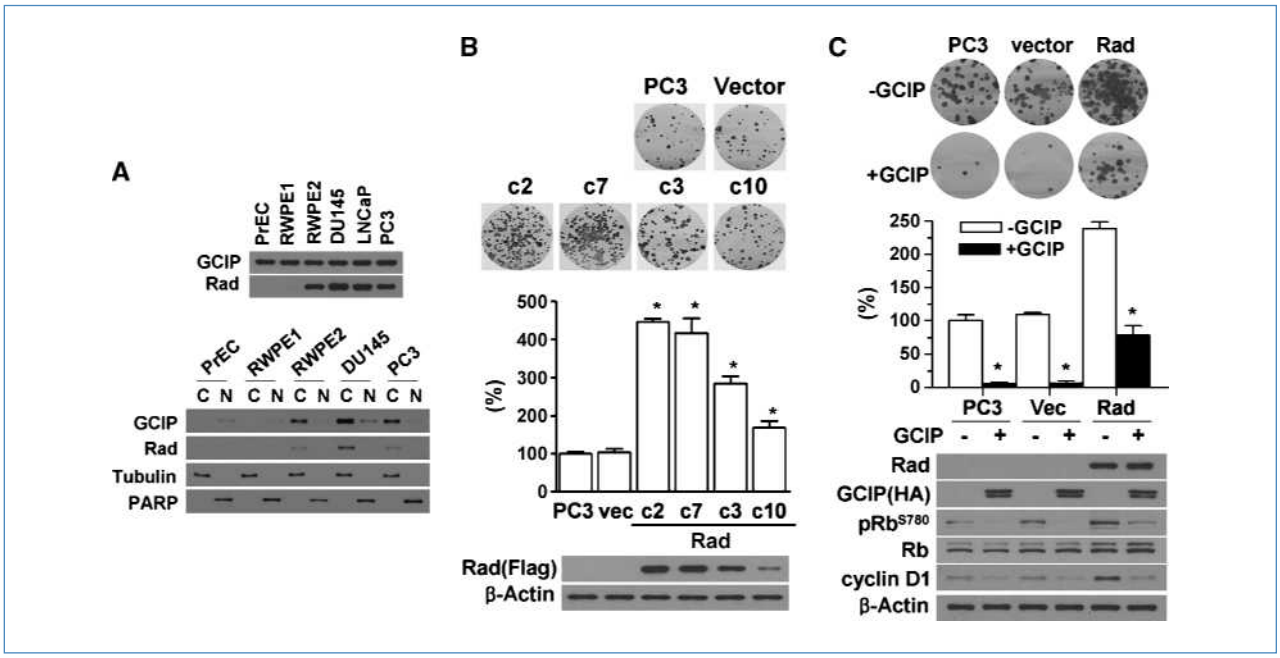

Figure 5. Rad modulates transformation and long-term colony formation of PC-3. A, expression of GCIP and Rad in normal (PrEC), immortalized (RWPE1), and transformed (RWPE2) human prostate cell lines, as well as in two prostate cancer–derived cell lines (DU145 and PC3). Top, equal amounts of protein (30 μg) were subjected to SDS-PAGE and Western blotting. Bottom, the nuclear (N) and cytoplasmic (C) fractions from indicated cells were analyzed by Western blotting to determine the distribution of GCIP and Rad. Cell lysates were prepared from either 2×10^6 (PrEC, RWPE1, and RWPE2) or 1×10^6 (DU145, PC3) cells. All fractions were adjusted to 100 μL and equal volumes were subjected to SDS-PAGE. B, a Rad expression level–dependent increase in colony formation. Stable PC-3 cell clones (2×10^2) were seeded in a 60-mm dish. After incubation for 2 wk, the cells stained with crystal violet were counted under phase-contrast microscopy. Rad expression was analyzed by Western blotting. *, $P < 0.05$, versus siC. C, abrogation of Rad-induced colony formation, cyclin D1 expression, and Rb phosphorylation by overexpression of GCIP. Stable PC-3 cell clones were transiently transfected with empty control vector or pHA-GCIP. Colony formation, cyclin D1 expression, and Rb phosphorylation were tested as described above. *, $P < 0.05$, versus empty vector.

clones (C2 and C20) compared with the empty vector control (V) cells. In contrast, the protein levels of pRb appeared unchanged across all tested cells. These results suggest that Rad may increase carcinogenesis by inhibiting the GCIP-mediated downregulation of cyclin D1. Rad-overexpressing cells showed a significant increase in the cell proliferation compared with its empty vector–transfected cells (Fig. 4C, bottom). A model based on our studies is presented in Fig. 4D.

Rad modulates long-term colony formation and telomerase activity

When we determined the levels/localization of Rad and GCIP in normal, immortalized, and transformed human prostate cell lines, including prostate cancer–derived cell lines, we observed that the cellular Rad levels increased with malignant progression (Fig. 5A, top). Furthermore, Rad expression caused the majority of the expressed GCIP to shift from the nucleus to the cytoplasm (Fig. 5A, bottom). To examine whether ectopic expression of Rad affects long-term colony formation and telomerase activity, we established PC-3 clones stably overexpressing Rad and a negative control stably containing the empty vector. Interestingly, our results revealed that colony formation and telomerase activity was significantly and dose-dependently higher in Rad-overexpressing cells relative to controls (Supplementary Fig. S6A and B; Fig. 5B). Furthermore, overexpression of GCIP abrogated Rad-induced colony formation, cyclin D1 expression, and Rb phosphorylation (Fig. 5C).

Rad knockdown decreases *in vivo* tumorigenesis

Then we compared the tumor formation of stable Rad-transfectant PC-3 and the control cells after s.c. implantation of cells into athymic nude mice. Rad-expressing cells formed tumor in 12 of 15 mice, whereas control cells formed none of five mice during 6 weeks after the transplantation ($P = 0.0036$; Supplementary Table S1). Our results also revealed that tumorigenesis was significantly and dose-dependently higher in Rad-overexpressing cells than in controls ($P = 0.0104$, t test comparing vector to Rad-10; Fig. 6A). Lastly, we investigated whether Rad knockdown could suppress tumor formation *in vivo*. When PC-3 cells transfected with siRad or siC were transplanted s.c. into athymic nude mice, the control cells formed tumors with an average size of 424 ± 68 mm^3 over 6 weeks. In contrast, siRad-transfected cells developed tumors that averaged 93 ± 28 mm^3 in size during the same period ($P = 0.0131$; Fig. 6B). More interestingly, in a tumor treatment model, the preestablished tumors progressed much more slowly after injecting siRad twice, which has been introduced

Downloaded from cancerres.aacrjournals.org on April 20, 2017. © 2010 American Association for Cancer Research.

Published OnlineFirst May 11, 2010; DOI: 10.1158/0008-5472.CAN-09-3791

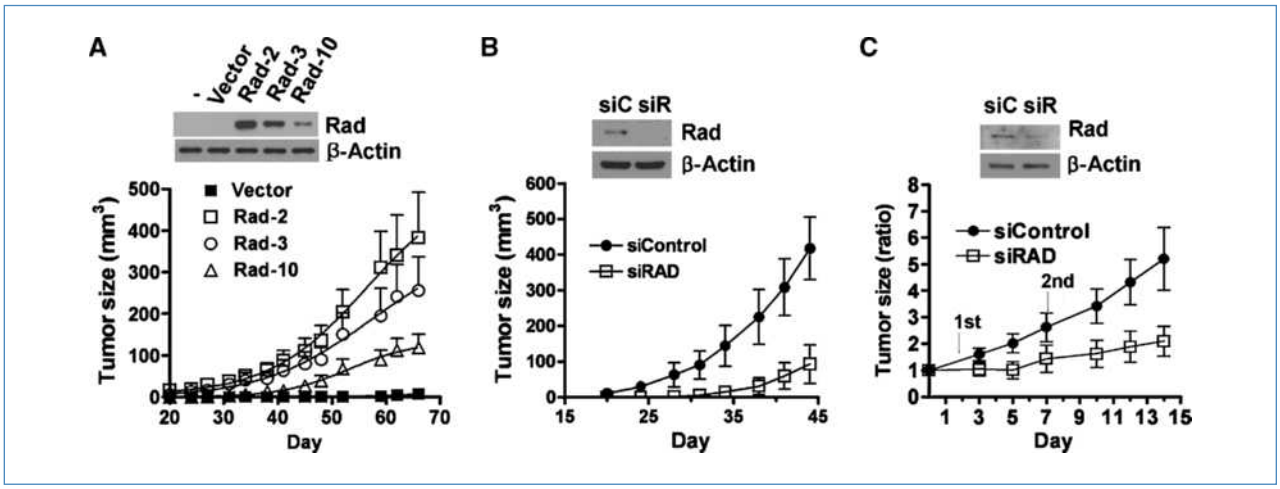

Figure 6. Rad-mediated control of *in vivo* tumorigenesis. A, effect of Rad expression level on tumor growth *in vivo*. For each injection, stable PC-3 cell clones were implanted s.c. into the flanks of 4-wk-old female athymic *nu/nu* mice. Five mice were used for each group (points, mean; bars, SEM). B, effect of Rad knockdown on tumor growth in nude mice. For each injection, PC-3 cells were transfected with 50 nmol/L Rad-targeting (siRad) or control siRNAs (siC) and implanted s.c. (n = 10). Points, mean; bars, SD. C, effect of intratumoral siRad injection on the growth of established tumors. When tumors reached an average size of 40 to 50 mm^3 (~4 wk), the mice received two (day 1 and 7) intratumoral injections of siRNA as a mixture of siRNA (50 nmol/L) in 100 μL of Effectene per injection (n = 10). Points, mean; bars, SD. Top, Western blot shows Rad expression in representative samples.

directly into the tumors (P = 0.0064; Fig. 6C), which strongly suggested that Rad could be an effective molecular target for cancer therapy.

Discussion

Senescence, which is defined as an irreversible growth arrest, is an important response by solid tumors following conventional chemotherapy or γ-irradiation. Conversely, escape from therapy-induced cellular senescence may form the basis of cancer recurrence or progression (17, 30, 31). To improve our understanding of how malignant cells escape senescence, we sought to define some of the genes that control cell cycle arrest. In a cDNA microarray hybridization analysis, we found that DNA damage–induced cell cycle arrest selectively inhibited a set of genes that included Rad. We subsequently found that Rad knockdown alone could induce cell growth arrest, which seemed to occur through senescence-like cell cycle arrest, but not cell death, in multiple cancer cells. Intriguingly, Rb, p53, and p16 were not required for siRad-induced cell cycle arrest. Indeed, among the tested cell lines, DU145 cells (which are resistant to doxorubicin treatment and contain mutations in p53, pRb, and p16) and PC-3 cells (which do not have functional p53 or p16) both entered growth arrest following Rad knockdown.

To understand how Rad regulates the cell cycle, we searched for Rad-interacting proteins using a yeast two-hybrid system and HeLa cDNA library. Although Rad was previously reported to interact with nm23 (4), calmodulin (5), calmodulin-dependent protein kinase II (5), and tropomyosin (6), this is the first study to show that Rad is capable of modulating the cell cycle through an interaction with GCIP. Several previous studies have suggested that GCIP may function as a potential tumor suppressor in human cancers. For example, GCIP was shown to interact with cyclin D1 and inhibit its transcriptional activity (9), and also decrease Rb phosphorylation, thereby downregulating cell cycle progression (10, 12). Lack of GCIP promotes the occurrence of hepatocellular carcinoma, suggesting that the absence of GCIP can contribute to a higher tumor incidence (13, 14, 32), and overexpression of GCIP in cancer cells has been associated with marked inhibition of cell growth (11, 12). GCIP associates with nuclear protein p29 and appears to execute its tumor suppressive functions in the nucleus (33). Therefore, it is perhaps unsurprising that the cytoplasmic sequestration of GCIP by Rad is associated with decreases in the inhibition of the GCIP-mediated cyclin D1 activity and increased cell cycle progression.

Although amplification of the gene encoding cyclin D1 is frequently observed in human cancers (34), cyclin D1 protein overexpression is more common than its gene amplification (35), suggesting that additional mechanisms may exist to cause the overexpression of cyclin D1 in human cancers. Increased Rad expression has been observed in human cancers and has been associated with poor prognosis in breast cancer (4).

Here, we show that Rad can enhance cyclin D1 protein expression by inhibiting the GCIP-mediated downregulation of Rb phosphorylation (Fig. 4D). In view of the fact that GCIP is ubiquitously expressed in mammalian tissues, the increased expression of Rad may be an important factor contributing to the cyclin D1 overexpression frequently seen in cancer tissues. Furthermore, our findings indicate that Rad-overexpressing cells are resistant to growth arrest and can proliferate in the presence of DNA damage–inducing agent that would normally induce senescence. Finally, this work provides *in vivo* evidence of differential tumorigenesis according to Rad knockdown.

Downloaded from cancerres.aacrjournals.org on April 20, 2017. © 2010 American Association for Cancer Research.

Published OnlineFirst May 11, 2010; DOI: 10.1158/0008-5472.CAN-09-3791

In sum, we herein show for the first time that Rad interacts with GCIP and inhibits GCIP-mediated reductions of Rb phosphorylation and cyclin D1 expression, thereby contributing to tumorigenesis.

Disclosure of Potential Conflicts of Interest

No potential conflicts of interest were disclosed.

Grant Support

Grants from Samsung Biomedical Research Institute (C-A8-201) and (C-A8-401).

The costs of publication of this article were defrayed in part by the payment of page charges. This article must therefore be hereby marked *advertisement* in accordance with 18 U.S.C. Section 1734 solely to indicate this fact.

Received 10/14/2009; revised 02/26/2010; accepted 03/11/2010; published OnlineFirst 05/11/2010.

References

1. Reynet C, Kahn CR. Rad: a member of the Ras family overexpressed in muscle of type II diabetic humans. Science 1993;262:1441–4.
2. Maguire J, Santoro T, Jensen P, Siebenlist U, Yewdell J, Kelly K. Gem: an induced, immediate early protein belonging to the Ras family. Science 1994;265:241–4.
3. Bilan PJ, Moyers JS, Kahn CR. The Ras-related protein Rad associates with the cytoskeleton in a non lipid-dependent manner. Exp Cell Res 1998;242:391–400.
4. Tseng YH, Vicent D, Zhu J, et al. Regulation of growth and tumorigenicity of breast cancer cells by the low molecular weight GTPase Rad and nm23. Cancer Res 2001;61:2071–9.
5. Moyers JS, Bilan PJ, Zhu J, Kahn CR. Rad, and Rad-related GTPases interact with calmodulin and calmodulin-dependent protein kinase II. J Biol Chem 1997;272:11832–9.
6. Zhu J, Bilan PJ, Moyers JS, Antonetti DA, Kahn CR. Rad, a novel ras-related GTPase, interacts with skeletal muscle b-tropomyosin. J Biol Chem 1996;271:768–73.
7. Smith JR, Pereira-Smith OM. Replicative senescence: implications for *in vivo* aging and tumor suppression. Science 1996;273:63–7.
8. Chang BD, Broude EV, Dokmanovic M, et al. A senescence-like phenotype distinguishes tumor cells that undergo terminal proliferation arrest after exposure to anticancer agents. Cancer Res 1999;59:3761–7.
9. Xia C, Bao Z, Tabassam F, et al. GCIP, a novel human grap2 and cyclin D interacting protein, regulates E2F-mediated transcriptional activity. J Biol Chem 2000;275:20942–8.
10. Terai S, Aoki H, Ashida K, Thorgeirsson SS. Human homologue of maid: a dominant inhibitory helix-loop-helix protein associated with liver-specific gene expression. Hepatology 2000;32:357–66.
11. Yao Y, Doki Y, Jiang W, et al. Cloning and characterization of DIP1, a novel protein that is related to the Id family of proteins. Exp Cell Res 2000;257:22–32.
12. Ma W, Stafford LJ, Li D, et al. GCIP/CCNDBP1, a helix-loop-helix protein, suppresses tumorigenesis. J Cell Biochem 2007;100:1376–86.
13. Natrajan R, Louhelainen J, Williams S, Laye J, Knowles MA. High-resolution deletion mapping of 15q13.2-q21.1 in transitional cell carcinoma of the bladder. Cancer Res 2003;63:7657–62.
14. Ma W, Xia X, Stafford LJ, et al. Expression of GCIP in transgenic mice decreases susceptibility to chemical hepatocarcinogenesis. Oncogene 2006;25:4207–16.
15. Sonnenberg-Riethmacher E, Wüstefeld T, Miehe M, Trautwein C, Riethmacher D. Maid (GCIP) is involved in cell cycle control of hepatocytes. Hepatology 2007;45:404–11.
16. Stein GH, Beeson M, Gordon L. Failure to phosphorylate the retinoblastoma gene product in senescent human fibroblasts. Science 1990;249:666–9.
17. Oh YL, Hahm B, Kim YK, et al. Determination of functional domains in polypyrimidine-tract-binding protein. Biochem J 1998;331:169–75.
18. te Poele RH, Okorokov AL, Jardine L, Cummings J, Joel SP. DNA damage is able to induce senescence in tumor cells *in vitro* and *in vivo*. Cancer Res 2002;62:1876–83.
19. Gewirtz DA, Holt SE, Elmore LW. Accelerated senescence: an emerging role in tumor cell response to chemotherapy and radiation. Biochem Pharmacol 2008;76:947–57.
20. Dimri GP, Lee X, Basile G, et al. A biomarker that identifies senescent human cells in culture and in aging skin *in vivo*. Proc Natl Acad Sci U S A 1995;92:9363–7.
21. Alexander K, Hinds PW. Requirement for p27(KIP1) in retinoblastoma protein-mediated senescence. Mol Cell Biol 2001;21:3616–31.
22. Park C, Lee I, Kang WK. Influence of small interfering RNA corresponding to ets homologous factor on senescence-associated modulation of prostate carcinogenesis. Mol Cancer Ther 2006;5:3191–6.
23. Park C, Lee I, Kang WK. E2F-1 is a critical modulator of cellular senescence in human cancer. Int J Mol Med 2006;17:715–20.
24. Elmore LW, Di X, Dumur C, Holt SE, Gewirtz DA. Evasion of a single-step, chemotherapy-induced senescence in breast cancer cells: implications for treatment response. Clin Cancer Res 2005;11:2637–43.
25. Goldstein S, Moerman EJ, Fujii S, Sobel BE. Overexpression of plasminogen activator inhibitor type-1 in senescent fibroblasts from normal subjects and those with Werner syndrome. J Cell Physiol 1994;161:571–9.
26. Murano S, Thweatt R, Shmookler Reis RJ, Jones RA, Moerman EJ, Goldstein S. Diverse gene sequences are overexpressed in werner syndrome fibroblasts undergoing premature replicative senescence. Mol Cell Biol 1991;11:3905–14.
27. Saunders NA, Smith RJ, Jetten AM. Regulation of proliferation-specific and differentiation-specific genes during senescence of human epidermal keratinocyte and mammary epithelial cells. Biochem Biophys Res Commun 1993;197:46–54.
28. Chang TW, Chen CC, Chen KY, Su JH, Chang JH, Chang MC. Ribosomal phosphoprotein P0 interacts with GCIP and overexpression of P0 is associated with cellular proliferation in breast and liver carcinoma cells. Oncogene 2008;27:332–8.
29. Kitagawa M, Higashi H, Jung HK, et al. The consensus motif for phosphorylation by cyclin D1-4 is different from that for phosphorylation by cyclin A/E-Cdk2. EMBO J 1996;15:7060–9.
30. Roberson RS, Kussick SJ, Vallieres E, Chen SY, Wu DY. Escape from therapy-induced accelerated cellular senescence in p53-null lung cancer cells and in human lung cancers. Cancer Res 2005;65:2795–803.
31. Schmitt CA, Fridman JS, Yang M, et al. A senescence program controlled by p53 and p16INK4a contributes to the outcome of cancer therapy. Cell 2002;109:335–46.
32. Takami T, Terai S, Yokoyama Y, et al. Human homologue of maid is a useful marker protein in hepatocarcinogenesis. Gastroenterology 2005;128:1369–80.
33. Chang MS, Chang CL, Huang CJ, Yang YC. p29, a novel GCIP-interacting protein, localizes in the nucleus. Biochem Biophys Res Commun 2000;279:732–7.
34. Diehl JA. Cycling to cancer with cyclin D1. Cancer Biol Ther 2002;1:226–31.
35. Hosokawa Y, Arnold A. Cyclin D1/PRAD1 as a central target in oncogenesis. J Lab Clin Med 1996;127:246–52.

Downloaded from cancerres.aacrjournals.org on April 20, 2017. © 2010 American Association for Cancer Research.

Published OnlineFirst May 11, 2010; DOI: 10.1158/0008-5472.CAN-09-3791

Cancer Research
The Journal of Cancer Research (1916–1930) | The American Journal of Cancer (1931–1940)

AACR American Association for Cancer Research

A Novel Senescence-Evasion Mechanism Involving Grap2 and Cyclin D Interacting Protein Inactivation by Ras Associated with Diabetes in Cancer Cells under Doxorubicin Treatment

Inkyoung Lee, Seon-Yong Yeom, Sook-Ja Lee, et al.

Cancer Res Published OnlineFirst May 11, 2010.

Updated version	Access the most recent version of this article at: doi:10.1158/0008-5472.CAN-09-3791
Supplementary Material	Access the most recent supplemental material at: http://cancerres.aacrjournals.org/content/suppl/2010/05/10/0008-5472.CAN-09-3791.DC1

E-mail alerts	Sign up to receive free email-alerts related to this article or journal.
Reprints and Subscriptions	To order reprints of this article or to subscribe to the journal, contact the AACR Publications Department at pubs@aacr.org.
Permissions	To request permission to re-use all or part of this article, contact the AACR Publications Department at permissions@aacr.org.

Downloaded from cancerres.aacrjournals.org on April 20, 2017. © 2010 American Association for Cancer Research.